Vol 18 No 10, October 2009
1674-1056/2009/18(10)/4353–07

Chinese Physics B

© 2009 Chin. Phys. Soc.
and IOP Publishing Ltd

# Lattice Boltzmann simulation of fluid flows in two-dimensional channel with complex geometries*

Wen Bing-Hai(闻炳海), Liu Hai-Yan(刘海燕), Zhang Chao-Ying(张超英)†, and Wang Qiang(王 强)

*College of Computer Science and Information Engineering, Guangxi Normal University, Guilin* 541004, *China*

(Received 2 December 2008; revised manuscript received 12 March 2009)

Boundary conditions (BCs) play an essential role in lattice Boltzmann (LB) simulations. This paper investigates several most commonly applied BCs by evaluating the relative $L_2$-norm errors of the LB simulations for two-dimensional (2-D) Poiseuille flow. It is found that the relative $L_2$-norm error resulting from FHML's BC is smaller than that from other BCs as a whole. Then, based on the FHML's BC, it formulates an LB model for simulating fluid flows in 2-D channel with complex geometries. Afterwards, the flows between two inclined plates, in a pulmonary blood vessel and in a blood vessel with local expansion region, are simulated. The numerical results are in good agreement with the analytical predictions and clearly show that the model is effective. It is expected that the model can be extended to simulate some real biologic flows, such as blood flows in arteries, vessels with stenosises, aneurysms and bifurcations, etc.

**Keywords:** lattice Boltzmann method, complex boundary, fluid flow, numerical simulation
**PACC:** 4715, 4755

## 1. Introduction

It is well known that numerical simulation is an essential method to study complex fluid flows. In recent years, the lattice Boltzmann method (LBM) has been developed into an alternative and promising numerical scheme for simulating fluid flows and modeling physics in fluids.[1] Its accuracy and robustness have been broadly confirmed through numerical simulations of complex fluids such as turbulent flows,[2] multi-phase flows,[3,4] reaction–diffusion processes[5] and particle suspensions.[6−8] The LBM has been successfully applied to various hydrodynamic problems since it was proposed, and most of these applications are connected with relatively simple or regular boundaries, only a few references which discuss flow problems with little more complicated boundaries can be found.[6−9] However, real fluid systems in nature usually have complex or arbitrary and irregular geometrical boundaries. In order to understand the details in the flows of real fluid systems, it is necessary to develop an LB model which can be used to simulate the fluid flows with complex geometrical boundaries.

In LB simulations, an accurate and efficient boundary condition (BC) is, to some extent, as important as an accurate computation scheme itself, since the BC will obviously influence the accuracy and stability of the computation. In recent years, much effort has been spent in studying the BCs of the LBM, and a number of BCs have been proposed,[10−15] which, although stemming from different schemes, can successfully describe the boundary behaviors in LB simulations. As BCs play an essential role in LB simulations, an accurate and efficient BC for developing an LBM with complex boundaries is needed. In this paper we first investigate several most commonly applied boundaries by analyzing the relative $L_2$-norm errors in LB simulations for two-dimensional (2-D) Poiseuille flow. Based on these analyses, we select an optimal BC with which the error resulting from LB simulation is smaller than other BCs as a whole. Secondly, with the selected BC, an LB model is developed which can be used to simulate fluid flows in 2-D channel with complex geometries. Thirdly, the model is used to simulate several flows with complex boundaries to test its validity, including flows between two inclined plates, in a large pulmonary blood vessel and in a blood vessel with local expansion region. For the flows with curved geometrical boundaries, the boundaries will obviously change the distributions of the velocity and pressure along the channel axis. Therefore, the distributions of the velocity and pressure in our

*Project supported by the National Natural Science Foundation of China (Grant No 10765002), and Guangxi Natural Science Foundation (Grant No 0542045).
†Corresponding author. E-mail: zhangcy@gxnu.edu.cn

simulations are evaluated not only on the cross section vertical to the flow direction, but also along the channel axis.

# 2. LB model with 2-D complex geometrical boundaries

## 2.1. LBM with a single relaxation time

In the early 1990s, Qian[16] and Chen[17] proposed the LBM with a single relaxation time approximation. The relevant LB equation (LBE) is given by

$$\frac{\partial f_i}{\partial t} + \boldsymbol{e}_i \cdot \boldsymbol{\nabla} f_i = -\frac{1}{\tau}(f_i - f_i^{(\mathrm{eq})}),$$
$$(i = 0, 1, 2, \ldots, N-1), \tag{1}$$

where $\boldsymbol{e}_i$ is a discrete velocity, $f_i$ is the particle distribution function with the velocity $\boldsymbol{e}_i$, $f_i^{(\mathrm{eq})}$ is the corresponding equilibrium distribution function, $N$ is the number of the different velocities in the model, $\tau$ is the relaxation time. Equation (1) is then discretized, in space $\boldsymbol{x}$ and time $t$, into

$$f_i(\boldsymbol{x} + \boldsymbol{e}_i\delta_t, t + \delta_t) - f_i(\boldsymbol{x}, t)$$
$$= -\frac{1}{\tau}\left[f_i(\boldsymbol{x}, t) - f_i^{(\mathrm{eq})}(\boldsymbol{x}, t)\right], \tag{2}$$

where $\delta_t$ is the duration of the time step. The LBM applies two essential steps, namely collision and streaming, to reveal the flow phenomena at the mesoscopic scale. Hence, the corresponding computations of Eq.(2) are performed as

Collision:

$$\tilde{f}_i(\boldsymbol{x}, t) - f_i(\boldsymbol{x}, t) = -\frac{1}{\tau}\left[f_i(\boldsymbol{x}, t) - f_i^{(\mathrm{eq})}(\boldsymbol{x}, t)\right]; \tag{3}$$

Streaming:

$$f_i(\boldsymbol{x} + \boldsymbol{e}_i\delta t, t + \delta t) = \tilde{f}_i(\boldsymbol{x}, t), \tag{4}$$

where $f_i$ and $\tilde{f}_i$ denote pre-collision and post-collision states of the particle distribution functions, respectively. The macroscopic physics quantities can be solved by the distribution function $f_i$, such as density $\rho = \sum_i f_i$, momentum density $\rho\boldsymbol{u} = \sum_i f_i\boldsymbol{e}_i$, velocity $\boldsymbol{u} = (\sum_i f_i\boldsymbol{e}_i)/\rho$, etc.

## 2.2. Curved boundary condition

The curved BC plays an important part in LBM applications. As shown in Fig.1, a physical boundary locates at an arbitrary position between two adjacent grid sites and the side length of the grid is $\delta x$. The $\boldsymbol{x}_b$ and $\boldsymbol{x}_f$ denote the solid and fluid grid sites, respectively, $\boldsymbol{x}_w$ is the intersection of the physical boundary and the link between $\boldsymbol{x}_b$ and $\boldsymbol{x}_f$. $\boldsymbol{e}_i$ and $\boldsymbol{e}_{\bar{i}}$ stand for directions opposite to each other, which are defined as $\boldsymbol{e}_i = \boldsymbol{x}_b - \boldsymbol{x}_f$ and $\boldsymbol{e}_{\bar{i}} = -\boldsymbol{e}_i$, respectively. The fraction of an intersected link in the fluid region is $\Delta$, that is,

$$\Delta = |\boldsymbol{x}_f - \boldsymbol{x}_w|/|\boldsymbol{x}_f - \boldsymbol{x}_b|,\ 0 \le \Delta \le 1. \tag{5}$$

The BC is to solve $\tilde{f}_{\bar{i}}(\boldsymbol{x}_b, t)$ with different $\Delta$s, which is going to stream from $\boldsymbol{x}_b$ to $\boldsymbol{x}_f$ in the streaming step.

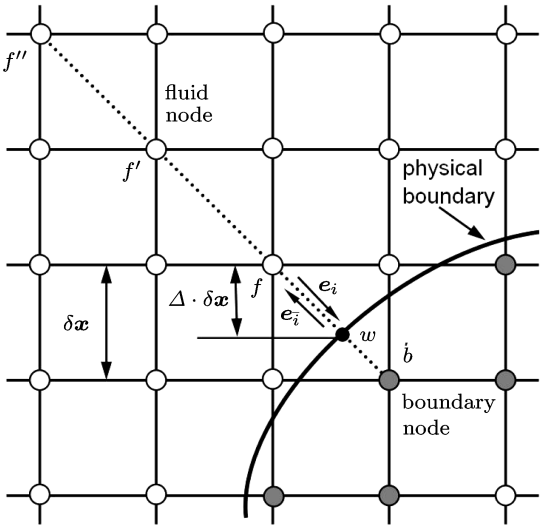



**Fig.1.** Layout of curved wall boundary.

Since BC is essential in LB simulations, an accurate and efficient BC is important for developing an LB model with complex geometrical boundaries. Therefore, an assessment scheme must be constructed in order to compare the errors caused by these curved BCs. For a channel with complex geometrical boundary, the distance between the boundary and the adjacent grid sites is arbitrary, that is, $\Delta$ can be any value between 0 and 1. However, the relaxation time is an important factor influencing the stability of the LB simulation. Thus, a suitable assessment scheme should be that the effects on errors resulting from both of $\Delta$ and $\tau$ can be considered as a whole. An optimal BC should produce small errors for different $\Delta$s and maintain stability in more wide regions of $\tau$ in LB simulations.

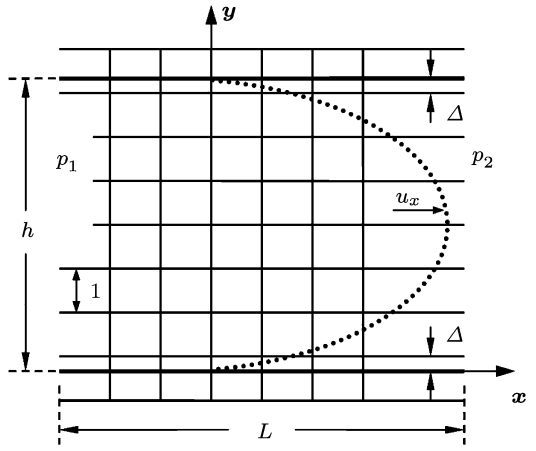



**Fig.2.** Lattice configuration in channel flow simulations.

A plane Poiseuille flow is a simple yet very useful fluid flow which can be analytically solved, and, hence, is widely used in studies of BCs.[10−15] In this paper, therefore, we will use the plane Poiseuille flows to investigate several widely applied curved BCs. As shown in Fig.2, the height of the channel is $h$, the distance between the physical boundary and the nearest grid line is $\Delta$ ($0 \le \Delta \le 1$), the pressures at the inlet and outlet are $p_1$ and $p_2$, respectively. For 2-D Poiseuille flow driven by a pressure gradient, the analytic solution is

$$\boldsymbol{u}_0(y) = -\frac{1}{2}\frac{\mathrm{d}p}{\mathrm{d}x}\frac{h^2}{\rho v}(\eta^2 - \eta), \tag{6}$$

where $\mathrm{d}p/\mathrm{d}x$ is the pressure gradient, $v$ is viscosity of the fluid, $\rho$ is the fluid density, and $\eta = y/h$. In order to evaluate the computational error of the LB simulation, the relative $L_2$-norm error is defined as follows:

$$E = \frac{\left\{ \int_0^h [\boldsymbol{u}(y) - \boldsymbol{u}_0(y)]^2 \mathrm{d}y \right\}^{1/2}}{\left\{ \int_0^h \boldsymbol{u}_0^2(y) \mathrm{d}y \right\}^{1/2}}. \tag{7}$$

It is obvious that $E$ is a function of both $\Delta$ and $\tau$. To consider the relative errors of the LB simulations with different $\Delta$s as a whole, we define a total error as

$$G_N = \left( \sum_i^N E^2(\Delta_i, \tau) \right)^{1/2},$$
$$\Delta_i = i/N, \quad i = 0, 1, \ldots N. \tag{8}$$

In this work, six most commonly applied BCs are investigated based on the total error $G_N$, among them: 1) Two BCs based on fictitious equilibrium distribution function, proposed by Filippova and Häne,[10] Mei and Luo[11,12] are treated as a single one scheme named FHML, because these two schemes are complementary to each other on the stability regions; 2) Two BCs are based on partitioned interpolation, proposed by Bouzidi, Firdaouss and Lallemand[13,14] (BFL1 denotes the linear interpolation and BFL2 the quadratic interpolation); 3) Two BCs are based on unified interpolation, proposed by Yu, Mei and Shyy[15] (YMS1 denotes the linear interpolation and YMS2 the quadratic interpolation). The LB simulations with these 6 BCs for plane Poiseuille flow are performed, and the corresponding evaluated $G_N$s are given in Fig.3. It is shown that the total error $G_N$ caused in the LB simulation with FHML is averagely the smallest in the whole range of $\tau$. Therefore, in the following simulations with complex boundaries, FHML will be applied as the BC of the LBM.

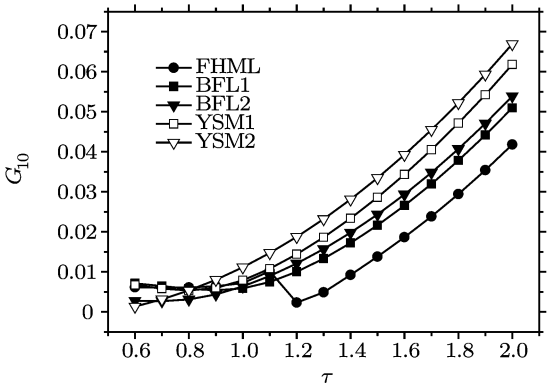



**Fig.3.** $G_{10}$ profile.

## 2.3. LB model with 2-D complex geometrical boundaries

We begin with the two-dimensional nine-velocity model (D2Q9), the particle equilibrium distribution function can be written as

$$f_i^{(\mathrm{eq})} = \rho\varpi_i \left[ 1 + \frac{3}{c^2}(\boldsymbol{e}_i \cdot \boldsymbol{u}) + \frac{9}{2c^4}(\boldsymbol{e}_i \cdot \mathbf{u})^2 - \frac{3}{2c^2}\boldsymbol{u}^2 \right], \tag{9}$$

where $\varpi_0 = 4/9$, $\varpi_{1,2,3,4} = 1/9$, $\varpi_{5,6,7,8} = 1/36$. Basing on this equilibrium distribution function and applying the Chapman–Enskog expansion, we can recover exactly the continuity equation and the Navier–Stockes equations at the second-order approximation from the LB Eq.(2), if the density variation is sufficiently small. So, by evolving the LB equation in the form of D2Q9 model together with the FHML BC, we can simulate the spatiotemporal behaviors of the fluid flow with complex geometrical boundaries.

# 3. Numerical results and discussion

## 3.1. Simulation of flow between two inclined plates

As illustrated in Fig.4, unlike in a flow between two parallel plates, the pressure gradient along the flowing direction is not a constant in the flow between two inclined plates:[18]

$$p_x = p_1 - (p_1 - p_2)\frac{(h_1/h)^2 - 1}{(h_1/h_2)^2 - 1}, \qquad (10)$$

where $h_1$, $h_2$ and $p_1$, $p_2$ are the heights and pressures at the channel inlet and outlet, respectively. The flow between the two inclined plates with $L = 180$, $h_1 = 37$ and $h_2 = 21$ is simulated with our LB model. The numerical results of the axial velocity and pressure are given in Fig.5. In the same picture, the corresponding analytical solution is also plotted. It is clearly shown that the axial velocity of the flow increases when the height decreases and the pressure decreases with $x$, but the decreasing rate of the pressure is slower than that in the plane Poiseuille flow. The numerical results of both axial velocity and pressure are in excellent agreement with those of the analytical solutions.

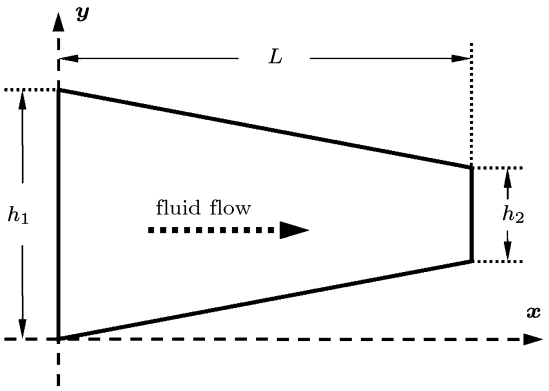



**Fig.4.** Layout of two inclined plates.

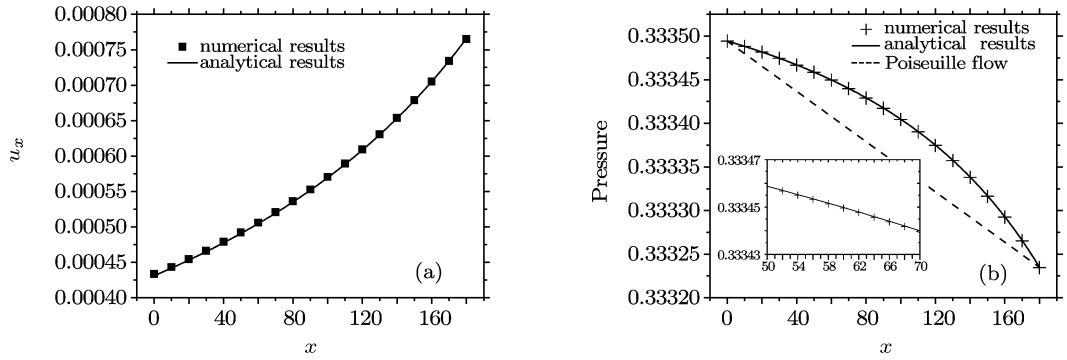



**Fig.5.** Simulations of flow between two inclined plates. (a) Velocity profile at the central axis; (b) Pressure profile at the axis.

## 3.2. Simulation of flow in a big pulmonary blood vessel

We perform simulation of a flow in a big pulmonary blood vessel, which can be approximatively considered as a long, thin, smooth and non-uniform tube with length $L$. The $x$ axis is set along with the axial direction of the blood vessel. For a big pulmonary blood vessel, the relationship of the pressure $p(x)$ with width $a(x)$ can be represented as[19,20]

$$p(x) - p_0 = \alpha(a(x) - a_0), \qquad (11)$$

where $a_0$ is the width in which the pressure inside is fixed to $p_0$ and $\alpha$ is a compliant constant. Since the pipe is long, thin and smooth under deformation, the flow in it can be approximated to a plane Poiseuille flow. By using the volume-flow definition, Eqs.(6) and (11), we obtain a theoretical formula for the width $a(x)$ and pressure $p(x)$:

$$a^4(x) - a^4(0) = -48vQ/\alpha, \qquad (12)$$

$$[a_0 + (p(x) - p_0)/\alpha]^4 - [a_0 + (p(0) - p_0)/\alpha]^4 = -48vQx/\alpha, \qquad (13)$$

where $Q$ is the volume-flow rate, which is constant throughout the vessel.

In our numerical simulation, $p_0 = 0.333$, $a_0 = 20$, $\tau = 0.8$, $L = 200$, and the fluid flows from left to right. Figure 6 illustrates the width of a blood vessel under Eq.(11). The numerical results of the axial velocity and pressure are shown in Fig.7. We can easily see that, in a narrowing pulmonary blood vessel, the fluid velocity shows a gradual increase and the pressure a gradual decrease. The simulation results are in good agreement with the analytical predictions.

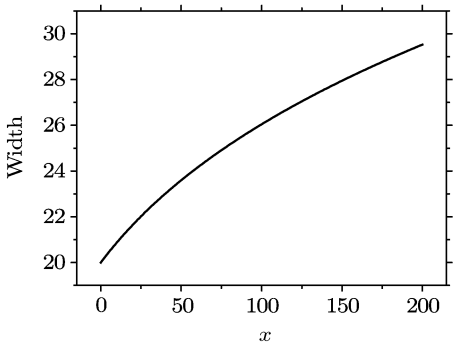



**Fig.6.** Width profile of blood vessel.

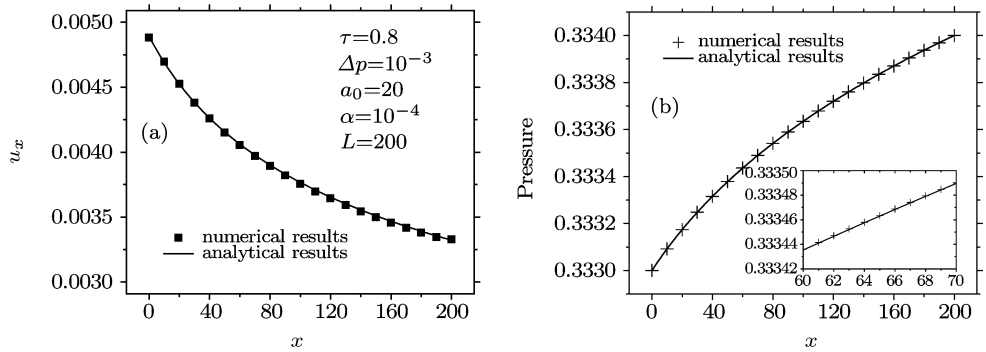



**Fig.7.** Simulations of flow in a big pulmonary blood vessel. (a) Blood velocity profile. (b) Blood pressure profile.

## 3.3. Simulation of flow in a blood vessel with local expansion region

The numerical simulations have been widely applied to diagnose and treat some vascular diseases, such as artery hemangioma. As a third sample, we consider a model of a blood vessel with local expansion region, just like a section of vessel with a hemangioma. The local expansion region of a blood vessel can be approximately represented as cosine curves (shown in Fig.8(a)):[21]

$$\frac{r}{r_0} = \begin{cases} 1, & x < x_1 \quad \text{or} \quad x > x_2, \\ 1 + \delta/(2r_0)(1 + \cos(\pi x/x_0)), & x_1 \le x \le x_2. \end{cases} \tag{14}$$

Assuming that the fluid flow satisfies the "slow-flow" condition, the pressure difference at inlet and outlet can be obtained by the flow continuity equation and the volume-flow rate definition

$$\Delta p_x = 8vQ/(\pi r_0^4) * G(x), \tag{15}$$

where $v$ is the viscosity of the fluid, and $G(x)$ is defined as

$$G(x) = \int_0^x \left(\frac{r}{r_0}\right)^{-4} \mathrm{d}x = \begin{cases} x, & x < x_1, \\ x_1 + \displaystyle\int_{x_1}^{x} \left(\frac{r}{r_0}\right)^{-4} \mathrm{d}x, & x_1 \le x \le x_2, \\ x + x_1 + \displaystyle\int_{x_1}^{x_2} \left(\frac{r}{r_0}\right)^{-4} \mathrm{d}x, & x > x_2. \end{cases} \tag{16}$$

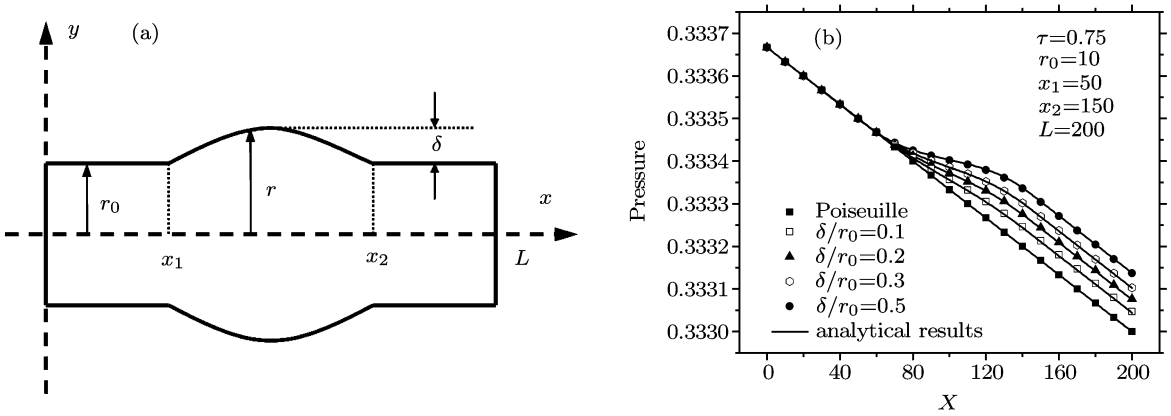



**Fig.8.** Simulations of blood vessel with local expansion region. (a) Layout of blood vessel with local expansion region. (b) Pressure profile with different $\delta$.

Denoting $p_0$ as the pressure at the inlet, we can derive the analytical solution of the pressure at $x$ of the vessel

$$p_x = p_0 - 8vQ/(\pi r_0^4) * G(x). \tag{17}$$

Initially, the flow field is configured as $L = 200$, $r_0 = 10$, $x_1 = 50$, $x_2 = 150$ and $p_0 = 0.33367$. At first, the Poiseuille flow ($\delta = 0$) with $\mathrm{d}p/\mathrm{d}x = 1e-5$ is simulated, and then the flows with different $\delta$s ($\delta/r_0 = 0.1, 0.2, 0.3, 0.5$) are also simulated with the pressures at the outlet being set to the values which keep the pressures equal to those in the Poiseuille flow before the expansion region. The simulated results are shown in Fig.8(b), in which the corresponding analytical solutions are also plotted. It is found that the fluid pressure increases gradually within the expansion region ($x_1 \leq x \leq x_2$) and remains high in the rest part ($x > x_2$). The phenomenon shows that the fluid pressures in the expansion region are higher than those in a pipe without expansion and the increase of the pressures grows with the expansion scale. The simulation results are in good agreement with the analytical results.

# 4. Conclusion

In this paper, we investigated several most commonly applied curved BCs, namely, FHML, BFL1, BFL2, YMS1 and YMS2, by evaluating the relative $L_2$-norm error resulting from the LB simulations for 2-D Poiseuille flow, and found that the FHML BC causes smaller errors in the simulation than the rest BCs. Basing on the FHML BC, we developed an LB model which is suitable for simulating 2-D fluid flow with complex geometrical boundaries, and then performed some typical simulations. The accuracy and validity of the model are confirmed through the good agreement between numerical results and analytical predictions. It is expected that the model can be extended to simulate some biologic flows, such as blood flows in arteries, vessels with stenosises, aneurysms and bifurcations, etc. Considering the importance of BC in LB simulations, we will look for more accurate and efficient BCs in order to improve the accuracy and stability of the simulations, and apply them into the simulations of 3-D fluid flows with complex geometrical boundaries.

# References

[1] Chen S Y and Doolen G D 1998 *Ann. Rev. Fluid Mech.* **30** 329

[2] Eggels J G M 1996 *Int. J. Heat Fluid Flow* **17** 307

[3] He X Y and Doolen G D 1997 *Phys. Rev.* E **56** 434

[4] Fang H P, Fan L W, Wang Z W, Lin Z F and Qian Y H 2001 *Int. J. Mod. Phys.* B **15** 1287

[5] Chen S Y, Dawson S P, Doolen G D, Janecky D R and Lawniczak A 1995 *Comp. Chem. Eng.* **19** 617

[6] Zhang C Y, Shi J, Tan H L, Liu M R and Kong L J 2004 *Chin. Phys. Lett.* **21** 1108

[7] Qi D W 1999 *J. Fluid Mech.* **41** 385

[8] Li H B, Fang H P, Lin Z F, Xu S X and Chen S Y 2004 *Phys. Rev.* E **69** 031919

[9] Kang X Y, Ji Y P, Liu D H and Jin Y J 2008 *Chin. Phys.* B **17** 1042
[10] Filippova O and Hänel D 1998 *Comput. Phys.* **147** 219
[11] Mei R W, Luo L S and Shyy W 1999 *Comput. Phys.* **155** 307
[12] Mei R W, Shyy W, Yu D Z and Luo L S 2000 *Comput. Phys.* **161** 680
[13] Bouzidi M, Firdaouss M and Lallemand P 2001 *Phys. Fluids* **13** 3452
[14] Lallemand P and Luo L S 2003 *Comput. Phys.* **184** 406
[15] Yu D Z, Mei R W and Shyy W 2003 *AIAA* (New York) 2003-0953
[16] Qian Y H, Humieres D D and Lallemand P 1992 *Europhys. Lett.* **17** 479
[17] Chen S Y, Chen H D and Martine D O 1991 *Phys. Rev. Lett.* **67** 3776
[18] Lin J Z, Ruan X D and Chen B G 2005 *Fluid Mech.* (Beijing: Tsinghua University Press) p267 (in Chinese)
[19] Fung Y C 1997 *Biomechanics Circulation* (Berlin: Springer-Verlag) p118
[20] Fang H P, Lin Z F and Wang Z W 1998 *Phys. Rev.* E **57** 25
[21] Lu L and Chen Y 2001 *Journal of Medical Biomechanics* **16** 27 (in Chinese)